

## Article

# Health State Prediction of Aero-Engine Gas Path System Considering Multiple Working Conditions Based on Time Domain Analysis and Belief Rule Base

Xiaojing Yin <sup>1</sup>, Guangxu Shi <sup>1</sup>, Shouxin Peng <sup>1</sup>, Yu Zhang <sup>1</sup>, Bangcheng Zhang <sup>1,\*</sup> and Wei Su <sup>2</sup>

<sup>1</sup> School of Mechatronic Engineering, Changchun University of Technology, Changchun 130012, China; yinxiaojing@ccut.edu.cn (X.Y.); 2201901020@stu.ccut.edu.cn (G.S.); 2201901051@stu.ccut.edu.cn (S.P.); 2202001105@stu.ccut.edu.cn (Y.Z.)

<sup>2</sup> School of Aeronautical Engineering, Jilin Institute of Chemical Technology, Jilin 132000, China; sw@jict.edu.cn

\* Correspondence: zhangbangcheng@ccut.edu.cn

**Abstract:** The gas path system is an important part of an aero-engine, whose health states can affect the security of the airplane. During the process of aircraft operation, the gas path system will have different working conditions over time, owing to the change of control parameters. However, the different working conditions which change the symmetry of the system will affect parameters of the health state prediction model for the gas path system. The symmetry of the system will also change. Therefore, it is important to consider the influence of variable working conditions when predicting the health states of gas path system. The accuracy of the health state prediction results of the gas path system will be low if the same evaluation standard is used for different working conditions. In addition, the monitoring data of the gas path system's health state feature quantity is huge while the fault data which can reflect the health states of the gas path system are poor. Thus, it is difficult to establish a health state prediction model only by using the monitoring data of the gas path system. In order to avoid problems, this paper proposes a health state prediction model considering multiple working conditions based on time domain analysis and a belief rule base. First, working condition is divided by using time domain characteristics. Then, a belief rule base (BRB) theory-based health state prediction model is built, which can fuse expert knowledge and fault monitoring data to improve modeling accuracy. The reference value of the feature is given by the fuzzy C-means algorithm in a model. To decrease the uncertainty of expert knowledge, the covariance matrix adaptive evolution strategy (CMA-ES) is used as the optimization algorithm. Finally, a NASA public dataset without labels is used to verify the proposed health state model. The results show that the proposed health prediction model of a gas path system can accurately realize health state prediction under multiple working conditions.

**Keywords:** variable condition; belief rule base (BRB); dividing the working condition; health state prediction; aero-engine gas path system



**Citation:** Yin, X.; Shi, G.; Peng, S.; Zhang, Y.; Zhang, B.; Su, W. Health State Prediction of Aero-Engine Gas Path System Considering Multiple Working Conditions Based on Time Domain Analysis and Belief Rule Base. *Symmetry* **2022**, *14*, 26. <https://doi.org/10.3390/sym14010026>

Academic Editors: Tomohiro Inagaki, Zhiwen Chen, Hao Luo and Chao Cheng

Received: 12 November 2021

Accepted: 22 December 2021

Published: 26 December 2021

**Publisher's Note:** MDPI stays neutral with regard to jurisdictional claims in published maps and institutional affiliations.



**Copyright:** © 2021 by the authors. Licensee MDPI, Basel, Switzerland. This article is an open access article distributed under the terms and conditions of the Creative Commons Attribution (CC BY) license (<https://creativecommons.org/licenses/by/4.0/>).

## 1. Introduction

An aero-engine is a kind of complex thermal mechanism, and its health states can affect the safe and stable flying of an aircraft [1]. The failure rate of a gas path system is the highest among many subsystems of aero-engines. According to incomplete statistics, the failure caused by a gas path system accounts for more than 90% of the total number of engine failures, and the maintenance cost of a gas path system accounts for more than 60% of the total maintenance cost [2]. Therefore, it is necessary to predict the health states of an aero-engine gas path system.

The health state prediction of the aero-engine gas path system is based on the current health and performance of the aero-engine gas path system [3]. Combined with its known characteristics and performance, environment, normal operation data, failure data and

other necessary information are used to predict the future health states of the gas path system [4].

There are many methods that can be used to predict the health states of an aero-engine gas path system, such as the Kalman filter method [5,6], grey theory [7–9], neural network method [10,11], support vector machine [12,13], analytic hierarchy process [14,15], hidden Markov model [16,17], and expert knowledge [18–20]. A two-way kernel extreme learning machine was proposed to predict the health states of aero-engine gas path system by one parameter [21]. The literature [22] can denoise the collected health state parameters and predict the health states of a gas path system by using the denoising health state parameters. The above model can predict the health states of the gas path system while the accuracy of the prediction results is low owing to the complex structure of a gas path system and the single health state feature.

The literature [23] proposed a hybrid recurrent process neural network which integrates multiple health state characteristics of an engine gas path system and improves its state monitoring accuracy under a single working condition. The literature [24] proposed a BP neural network based on phase space reconstruction under a single working condition, which integrates multiple health state features and improves the accuracy of aero-engine state prediction technology.

The aircraft will experience different operating states when in operation. The gas path system will be in different working conditions affected by the change of the aircraft operation states. The accuracy of the prediction result of the health states will be low if the influence of variable working condition is not considered.

The above health state prediction model can integrate multiple health state features of an engine gas path system which can significantly improve the prediction accuracy of the health state prediction model under a single working condition. However, the changing operation of an airplane will mean the gas path system operates in different working conditions. Thus it will lead to a health state prediction result without an explanation.

In order to establish the aero-engine gas system health prediction model and consider the influence of expert knowledge and multiple working conditions, the working condition division model should be combined with the BRB model to improve the accuracy of the gas system health prediction model. Therefore, this paper proposes an aero-engine gas path system health prediction model considering multiple working conditions. The model first classifies the aero-engine gas path system working conditions based on time domain characteristics and sets the conditions for different working conditions. Different ranges of reference values are used. Then the feature reference value is determined based on the fuzzy c-means method. According to the result of the above, the BRB is used to fuse the health state monitoring data and prior expert knowledge to realize the health state prediction of the aero-engine gas path system considering multiple working conditions. Finally, the covariance matrix adaptive evolution strategy (CMA-ES) is used as the optimization algorithm to optimize the initial parameters given by the experts.

This paper is organized as follows. In Section 2, the problem is described and formulated. In Section 3, health state prediction of aero-engine gas path system considering the multiple working conditions based on time domain analysis and belief rule basis proposed, and the detailed steps are described. Section 4 presents a case study. Section 5 discusses the advantages and disadvantages of the method. Finally, the conclusions are given in Section 6.

## 2. Problem Description

The gas path system will be in different working conditions when the aircraft is running, which is influenced by the control parameters' change [25]. The health state feature of the gas path system will be influenced in different degrees if the working condition is changing. In addition, there are many health state features for the gas path system while the fault data, which can reflect the health states of the gas path system, are limited. Based on the above discussion, this paper proposes a health state prediction

model which predicts the health states of the gas path system under changeable working conditions to solve the following problems.

**Problem I.** The gas path system will be in different working conditions with the continuous change of aircraft operation states  $l_i \in L, i = 1, 2, \dots, m$ , where  $l_i$  is the different working condition,  $L$  is the set of all the working conditions,  $m$  is the number of working conditions. The health states of the gas path system will be affected by the control parameters in different degrees. The accuracy of the health state prediction result will be low if the same criterion  $C$  is used to predict the health states of the gas path system in all working conditions. Therefore, the key of problem 1 is how to identify the working condition by using the monitoring data recorded by the sensor and then sets a different criterion  $C_i$  for different working condition based on the above research.

**Problem II.** The structure of gas path system is very complex with many health state features  $X_i$  which can reflect its health states, such as high pressure rotor vibration deviation, low pressure rotor speed deviation and so on. However, the fault monitoring data  $X = (x_1, x_2, \dots, x_n)$  is limited, where  $X_i$  is health state feature,  $x_i$  is the fault monitoring data. However, the accuracy of health state prediction can be improved by combining fault monitoring data and expert knowledge  $E = (E_1, E_2, \dots, E_n)$ , where  $E$  is expert knowledge vector, and  $E_i$  is the parameter of expert knowledge vector. Therefore, the key to problem 2 is how to use a small amount of effective health state monitoring data combined with expert knowledge to establish a nonlinear model:

$$y(t) = \{(D_z, \beta_z)\} = f(x_1(t), x_2(t), \dots, x_n(t), L, E) \quad (1)$$

where,  $y(t)$  is the health state prediction results of aero-engine gas path system.  $f$  is a non-linear function, and represents the relationship between the system characteristics and the health states of the aero-engine gas path system.  $D$  denotes the health states of the aero-engine gas path system.  $\beta_z$  is the belief degree assessed to  $D_z$ , and  $z = 1, 2, \dots, Z$ .

For example, except for the condition of normal states and failure states, there is a sub-health condition in the aero-engine gas path system that can be expressed as:

$$D = \{(D_0) \text{Normal}, (D_1) \text{well}, (D_3) \text{medium}, (D_4) \text{general}, (D_5) \text{low}\} \quad (2)$$

If the aero-engine gas path system is in low health condition, the belief degree of  $D$  can be described as:

$$D = \{(D_0, 0), (D_1, 0), (D_3, 0), (D_4, 0), (D_5, 1)\} \quad (3)$$

Due to the high reliability of the aero-engine gas path system, it is hard to obtain complete monitoring data. Then Problem 2 is how to establish the non-linear health estimation model using expert knowledge and some effective monitoring data.

### 3. Health Prediction Model of Gas Path System under Multiple Working Conditions

In order to solve the above two problems, this part proposes a health state prediction model of a gas path system considering changeable working conditions. This health state prediction model of the gas path system includes the following four parts: the first part is to divide the working conditions by calculating the time domain characteristics of the health state feature. The second part is to combine expert knowledge and fuzzy C mean to determine the reference value of the feature. The third part is the time series prediction of the gas path system monitoring data according to the resulting division of the working condition. In the fourth part, the BRB is used to predict the health states of gas path system by combining the fault monitoring data and expert knowledge under the different working condition. This is shown in Figure 1.

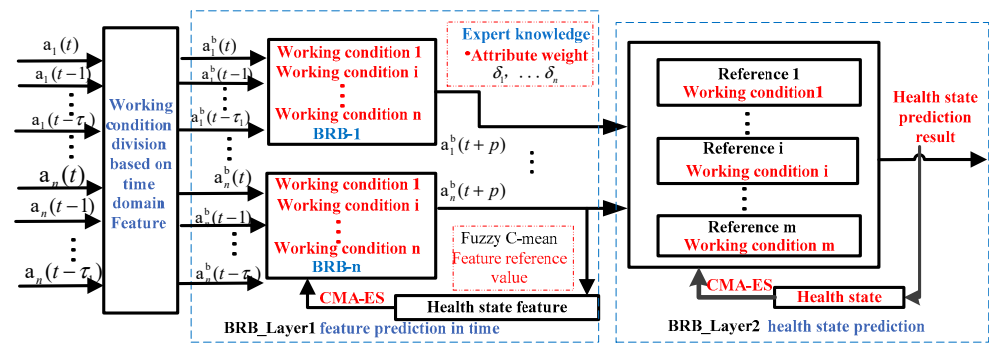


Figure 1. Health prediction model of gas path system with the changing working condition.

### 3.1. Dividing the Work Condition of Gas Path System Based on Domain Feature

The monitoring data are regarded as a sequence arranged in time order, which can reflect the information related to the working condition. The information which reflects the health states can be calculated through the fault monitoring data based on time domain features. There are some parameters such as average amplitude, mean square amplitude and so on [26].

Dimensional parameters related to the running states of the equipment can describe the actual movement of the equipment. The dimensionless parameter is not sensitive to the change of data amplitude and frequency which cannot reflect the operational states of the equipment [27]. Kurtosis can characterize the steepness of the peak of the probability density function of the data, and thus can characterize the size of the impact component in the monitoring data [28].

The gas path system’s health states will be impacted to different degrees with the impact of control parameters when the aircraft is running. Therefore, the gas path system will be in different working conditions. Since the kurtosis index can reflect the magnitude of the impact component of the monitoring data, the gas path system can be divided according to the prediction results of the kurtosis index. Therefore, the working conditions of the gas path system can be divided by calculating the kurtosis of the monitoring data. The specific process is as follows:

$$\mu_x = \lim_{T \rightarrow \infty} \frac{1}{T} \int_0^T [x(t) - \mu_x]^2 dt \tag{4}$$

$$\sigma_x^2 = \lim_{T \rightarrow \infty} \frac{1}{T} \int_0^T [x(t) - \mu_x]^2 dt \tag{5}$$

$$\beta = \frac{1}{T} \int_0^T [x(t) - \mu_x]^4 dt \tag{6}$$

$$K = \frac{\beta}{\sigma_x^4} \tag{7}$$

where,  $\mu_x$  represents the mean value of each group of data.  $\sigma_x^2$  represents the variance of each group of data.  $\beta$  represents the kurtosis of each group of data.  $K$  represents the kurtosis, which reflects the magnitude of the impact component of the signal. Finally, according to expert knowledge and time-domain feature analysis, the result of working condition division is obtained.

### 3.2. Health State Prediction Model Based on Belief Rule Base (BRB)

The BRB is used to predict the time series of the gas path system with expert knowledge and a small amount of effective monitoring data. The  $k$ -th rule is shown in Equation (8). According to the result of working condition division and expert knowledge, different

reference values are set for different working conditions of gas path system to improve the accuracy of the health state prediction result.

$$R_k^q: \text{ If } x(t-1) \text{ is } A_1^k \wedge x(t-2) \text{ is } A_2^k, \dots, \wedge x(t-\tau) \text{ is } A_\tau^k \\ \text{ Then } x(t) \text{ is } \{(D_1, \beta_{1,k}), \dots, (D_N, \beta_{N,k})\} \\ \text{ with a rule weight } \theta_k \text{ and attribute weight } \delta_1, \delta_2, \dots, \delta_N. \quad (8)$$

where, the  $R_k^q$  is  $k$ -th rule under the  $q$  working condition,  $x_n$  is the input health state feature of the gas path system,  $\tau$  the number of delay step,  $A_m^k (k = 1, 2, \dots, L)$  is the reference value of the  $m$ -th attribute in rule  $K$ ,  $p$  is the prediction step in the BRB prediction model,  $\beta_{j,k} (j = 1, 2, \dots, N, k = 1, 2, \dots, L)$  is belief degree of  $j$ -th result,  $D_j \in D$ .

There are many health state features which can reflect the health states of gas path system while the fault monitoring data are very limited. Thus it is necessary to use BRB to fuse multiple health state features of gas path system and expert knowledge improving the accuracy of health state prediction. The  $k$ -th rule of BRB to predict the health states is shown in Equation (9) [29]:

$$R_k^q: \text{ If } F_1 \text{ is } A_1^k \wedge F_2 \text{ is } A_2^k \\ \text{ Then the health state is } \{(D_0, \beta_{1,k}), (D_1, \beta_{2,k}), (D_3, \beta_{3,k}), (D_4, \beta_{4,k}), (D_5, \beta_{5,k})\} \\ \text{ with a rule weight } \theta_k \text{ and attribute weight } \delta_1, \delta_2, \delta_3, \delta_4, \delta_5 \quad (9)$$

where, the  $R_k^q$  is  $k$ -th rule under the  $q$  working condition,  $x(n) = [x_1(n), x_2(n), \dots, x_M(n)]^T$  is the vector composed of the engine gas path system health monitoring data input at  $n$  time,  $O(Y^1(n)) = h(x(n)) = \{(D_j, \hat{\beta}_j^1(n)), j = 1, 2, \dots, N\}$  is the corresponding output. The implementation process of the evidential reasoning algorithm [30] is shown as:

Step 3.2.1. The matching degree of the premise suggest that the matching degree of the feature quantity is calculated. The matching degree indicates the degree to which the premise attribute matches the rule. The matching degree of the premise attribute in  $k$ -th rule is calculated as follows:

$$a_i^k = \begin{cases} \frac{A_i^{l+1} - x_i}{A_i^{l+1} - A_i^l}, k = 1 (A_i^l \leq x_i \leq A_i^{l+1}) \\ 1 - a_i^k, k = l + 1 \\ 0, k = 1, \dots, N(k, l + 1) \end{cases} \quad (10)$$

where,  $A_i^l$  and  $A_i^{l+1}$  respectively represent the  $i$ -th premise attribute reference value in two neighboring rules.  $a_i^k$  represent the matching degree of the premise attribute in  $k$ -th rule.

Therefore, in the  $k$ -th rule, the matching degree can be calculated by:

$$a_k = \prod_{i=1}^T (a_i^k)^{\theta_i} \quad (11)$$

where,  $T$  represents the number of premise attributes included in the  $k$ -th rule;  $a_k$  represents the matching degree of the  $i$ -th input.

Step 3.2.2. Calculating activation weight. When the monitoring data are inputted to BRB, some rules are activated. After the matching degree has been obtained, the activation weight for the  $k$ th rule is calculated by:

$$\omega_k = \frac{\theta_k \alpha_k}{\sum_{l=1}^L \theta_l \alpha_l}, k = 1, 2, \dots, L \quad (12)$$

Step 2.2.3. Rule reasoning based on ER [30].

In the decision-making process of the BRB model, the ER algorithm is used for rule reasoning, and all the rules in the BRB are fused by the ER analysis algorithm.

First, the utility of the evaluation result is calculated by Equations (13) and (14).

$$\mu = \left[ \sum_{j=1}^N \sum_{k=1}^L (\omega_k \beta_{j,k} + 1 - \omega_k \sum_{i=1}^N \beta_{j,k}) - (M-1) \prod_{k=1}^L (1 - \omega_k \sum_{i=1}^N \beta_{j,k}) \right]^{-1} \quad (13)$$

$$\hat{\beta}_j = \frac{\mu \times \left[ \prod_{k=1}^L (\omega_k \beta_{j,k} + 1 - \omega_k \sum_{i=1}^N \beta_{j,k}) - \prod_{k=1}^L (1 - \omega_k \sum_{i=1}^N \beta_{j,k}) \right]}{1 - \mu \times \left[ \prod_{k=1}^L (1 - \omega_k) \right]} \quad (14)$$

where,  $\hat{\beta}_j$  is a function of the rule weight,  $\theta_k$  the attribute weight  $\bar{\delta}_i$ , and the confidence degree  $\beta_{j,k}$ .  $N$  represents the number of evaluation results  $\beta_j$ . represents the confidence of the output relative to the evaluation result  $D_j$

Assuming that the utility of the evaluation result  $D_j$  is  $\mu(D_j)$ , the expected utility of  $S(X)$  is:

$$\mu(S(X)) = \sum_{j=1}^M \mu(D_j) \beta_j \quad (15)$$

Therefore, the output of the health prediction model is:

$$\hat{y} = \mu(S(X)) \quad (16)$$

### 3.3. Dividing Feature Reference Values Based on Fuzzy C-Means

In the BRB model, the reference value of the feature is divided by expert knowledge. However, due to the uncertainty of the expert knowledge, which is not conducive to engineering practice, a new method is needed to determine the reference value of the feature.

Fuzzy mathematics is widely used in fuzzy control and artificial intelligence [31,32]. According to fuzzy thinking [33], reference values of the feature are obtained. Therefore, the fuzzy C-means value can be used to divide the reference value of the feature. The fuzzy C-means is show as:

$$FCM(c_1, c_2, \dots, c_c) = \sum_{i=1}^c \sum_{j=1}^n u_{ij}^m d_{ij}^2 \quad (17)$$

where,  $c$  is the number of feature reference values divided;  $n$  is the number of feature data;  $m$  is a weighted index;  $d_{ij} = \|x_j - c_i\|$ . Degree of membership  $u_{ij}$  is calculated by:

$$u_{ij} = \frac{1}{\sum_{k=1}^c \left( \frac{d_{ij}}{d_{kj}} \right)^{2/(m-1)}} \quad (18)$$

Feature reference values  $c_c$  is calculated by:

$$c_i = \frac{\sum_{j=1}^n u_{ij}^m x_j}{\sum_{j=1}^n u_{ij}^m} \quad (19)$$

Combining expert knowledge, all reference values of the feature can be determined by fuzzy C-means.

### 3.4. Parameter Optimization Based on Covariance Matrix Adaptive Evolution Strategy (CMA-ES) Optimization Algorithm

The initial parameters of the proposed model are given by experts while there is a certain degree of subjectivity in expert knowledge, which will lead to low accuracy of health

state prediction results. Therefore, this paper uses the CMA-ES optimization algorithm to optimize the initial parameters given by experts to further improve the accuracy of the gas path system health state prediction model [34,35].

The mean square error is used as the optimization target, and the construction of root mean square (MSE) objective function is as follows:

$$\zeta(V) = \frac{1}{T} \sum_{n=1}^T (y_n - \hat{y}_n)^2 \quad (20)$$

where,  $V = [\theta_k, \delta_i, \beta_{j,k}, \mu(D_j)]^T$  is the parameter vector of BRB,  $T$  is the number of monitoring data.

In order to make  $\hat{y}_n$  and  $y_n$  as close as possible, the following objective function is constructed  $\min_V \{\zeta(V)\}$ , which is shown as:

$$\begin{aligned} 0 &\leq \theta_k \leq 1, \quad k = 1, 2, \dots, L \\ 0 &\leq \bar{\delta}_i \leq 1, \quad i = 1, 2, \dots, N \\ 0 &\leq \beta_{j,k} \leq 1, \quad j = 1, 2, \dots, M; \quad k = 1, 2, \dots, L \\ \sum_{j=1}^M \beta_{j,k} &\leq 1, \quad k = 1, 2, \dots, L \end{aligned} \quad (21)$$

The boundary constraint problem can be solved by using CMA-ES optimization algorithm, which includes the following four steps.

Step 1: Sampling operation. Firstly, take the solution as the expected value, and then generate the normal distribution, which is shown in Equation (22), where  $V^0$  is the initial vector of BRB model.

$$V_q^{g+1} \sim \text{mean}^g + \eta^g N(0, C^g) \quad (q = 1, \dots, \lambda) \quad (22)$$

where,  $g$  is the  $g$ -th generation,  $\text{mean}$  is the central expectation,  $\eta$  is the number of step,  $C$  is the covariance matrix.

Step 2: Multi objective constraint. Constraints are transformed into functions of constrained objects. For example, the parameter vector contains the confidence of rule  $K$  in the BRB model, and. Under constraint conditions, the objective function is shown in Equation (23).

$$H_k(\beta_{j,k}) = \left| \sum_{j=1}^N \beta_{j,k} - 1 \right| \quad (23)$$

Step 3: Select and restructure. In this step, the central expectation will be offset to optimize the solution. In this step, the central expectation will be optimized. The optimal result is selected as the reference to continue the iterative update, which is shown in Equation (24).

$$\text{mean}^{g+1} = \sum_{i=1}^{\epsilon} \gamma_i V_{i:\lambda}^{g+1} \quad (24)$$

where,  $\gamma$  is the attribute weight and the sum of  $\gamma$  is 1,  $\lambda$  is the number of attribute weights,  $V_{i:\lambda}^{g+1}$  is the optimization result of the  $(g + 1)$  generation of layer- $i$ .

Step 4: Update the covariance matrix. according to Equations (25)–(28), the update process of the covariance matrix is as follows:

$$C^{g+1} = (1 - a_1 - a_\epsilon)C^g + a_1 b^{g+1} (b^{g+1})^T + a_\epsilon \sum_{i=1}^{\epsilon} \gamma_i \left( \frac{(V_{i:\lambda}^{g+1} - \text{mean}^g)}{\eta^g} \right) \left( \frac{(V_{i:\lambda}^{g+1} - \text{mean}^g)}{\eta^g} \right)^T \quad (25)$$

where,  $a_1$  and  $a_\varepsilon$  are learning factors,  $b$  is evolutionary path. The initial values of the evolutionary path are all set to 0, and  $b$  can be updated by Equation (26).

$$b^{g+1} = (1 - a_p)b^g + \sqrt{a_b(2 - a_b)\left(\sum_{i=1}^{\varepsilon} \gamma_i^2\right)^{-1} \frac{mean^{g+1} - mean^g}{\eta^g}} \quad (26)$$

where,  $a_b \leq 1$  is the relevant parameter of the evolutionary path,  $\eta$  is the step size, whose update process is shown in Equation (27).

$$\eta^{g+1} = \eta^g \exp\left(\frac{a_\eta}{d_\eta} \left(\frac{\|b_\eta^{g+1}\|}{E\|N(0, I)\|} - 1\right)\right) \quad (27)$$

where,  $d_\eta$  is the damping coefficient,  $E\|N(0, I)\|$  is the expected value of  $\|N(0, I)\|$ ,  $I$  is the identity matrix,  $a_\eta$  is the parameter of the evolution path  $b_\eta^g$ ,  $b_\eta^g$  can be obtained by Equation (28).

$$b_\eta^{g+1} = (1 - a_\eta)b_\eta^g + \sqrt{a_\eta(2 - a_\eta)\left(\sum_{i=1}^{\varepsilon} \gamma_i^2\right)^{-1} C^{(g) - \frac{1}{2}} \frac{m^{g+1} - m^g}{\eta^g}} \quad (28)$$

The following work process is repeated until the position meets the accuracy requirements. In this way, the optimization parameter  $V_{best}$  can be obtained.

#### 4. Case Study

This part selects two health state features of NASA public data without a time mark to verify the above established gas path system health state prediction model under the changing condition. It needs to consider the influence of environmental interference and sensor accuracy because this data set simulates the actual running states of aero-engine. Therefore, it is necessary to filter the data before health state prediction influenced by the environmental noise and sensor accuracy. Gaussian filtering is used to process these data [36]. The filtering results are shown in Figures 2 and 3.

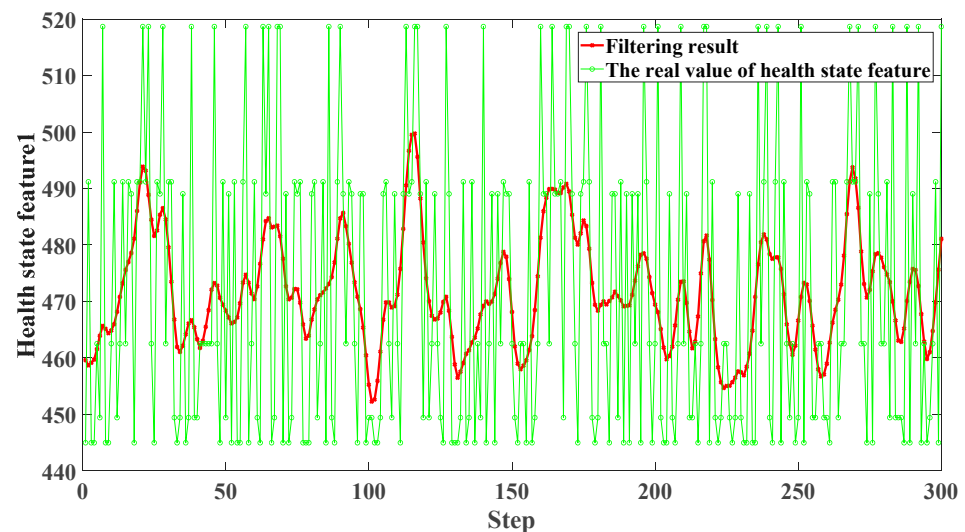


Figure 2. Health state feature 1 of gas path system.

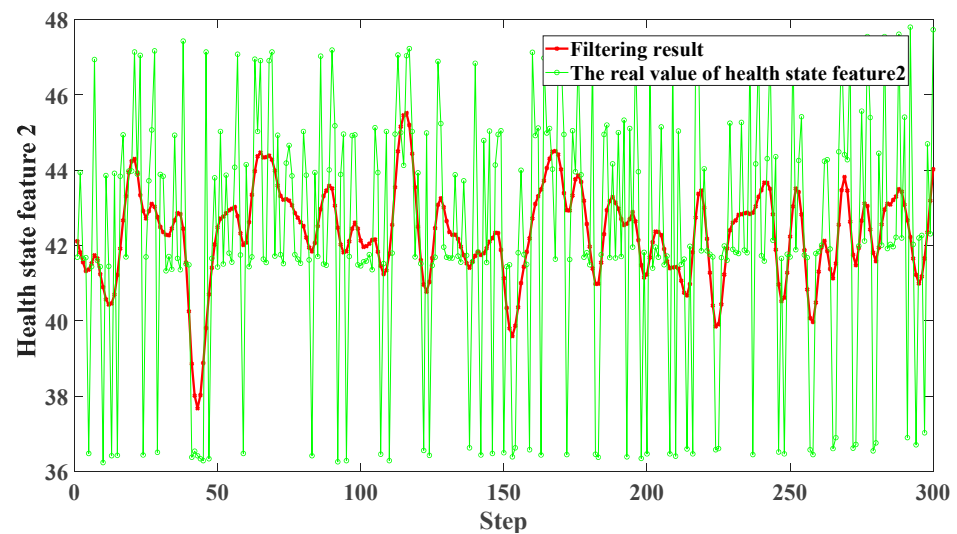


Figure 3. Health state feature 2 of gas path system.

#### 4.1. Dividing the Working Condition Based on Time Domain Feature

The health state feature obtained by sensors will be impacted in varying degrees by the influence of control parameters such as throttle size and lift angle. In addition, there is no obvious mark during the process of the dataset's acquisition. It is necessary to divide the working condition of the gas path system based on the time-domain feature of the health state feature. Thus the above two health state features are divided into a group every five monitoring data in time order and then calculate the kurtosis of them, which is shown in Figure 4.

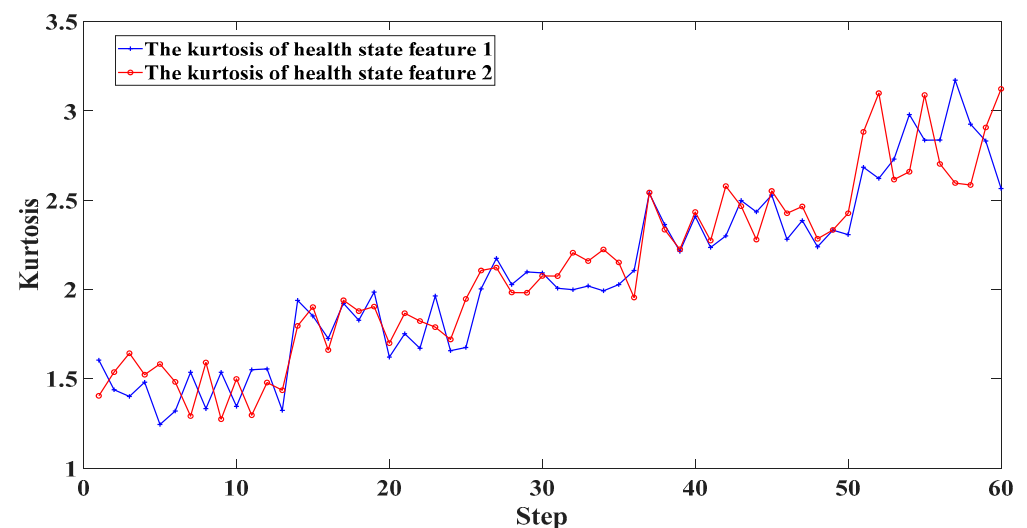


Figure 4. The kurtosis of health state features.

According to the kurtosis of the two health state features, the number of the gas path system's working condition is 5. These five different working conditions are changing with time, which are named working conditions 1 to 5.

#### 4.2. Health State Feature Prediction of Gas Path System Based on BRB

The BRB is used to fuse expert knowledge and a small amount of fault monitoring data to predict the health state feature in time series based on the dividing result of the working condition. According to the expert knowledge, there are four reference points "N", "M", "H" and "VH" respectively representing different meanings of "low", "medium", "high"

and “very high”. The number of reference values for each feature is set to 4, and  $c = 2$ . According to expert knowledge and fuzzy C-mean value, the feature reference value is calculated. The reference points of health state features under different working condition are shown in Table 1.

**Table 1.** The reference points of health state features under different working conditions.

Health State Feature 1				
Number	N	M	H	VH
1	456.18	465.11	480.22	499.79
2	448.35	468.86	486.32	504.39
3	452.18	463.52	486.66	496.21
4	453.77	459.48	475.45	489.38
5	454.50	462.32	477.56	498.47
Health State Feature 2				
1	37.67	40.52	42.72	44.31
2	41.24	42.21	44.23	45.52
3	39.59	41.61	43.31	44.51
4	39.85	41.22	42.81	43.48
5	39.97	41.35	43.11	44.03

The number of delay step is 2,  $\tau = 2$ , and the number of prediction step is 1,  $p = 1$  in this time series prediction model of an aero-engine gas path system. There are four reference points of  $x(t)$  and  $x(t - \tau)$ , thus there are 16 rules in the time series prediction model of the gas path system’s health state features. The initial parameters of the time series prediction model are given by expert knowledge, which is shown in Table 2.

**Table 2.** The initial parameters of time series prediction model.

Number	$x(t)$ AND $x(t-1)$	Belief Degree <sup>{D<sub>1</sub>,D<sub>2</sub>,D<sub>3</sub>,D<sub>4</sub>}</sup>
1	N AND N	(0, 0.5, 0.5, 0)
2	N AND M	(0.8, 0, 0.2, 0)
3	N AND H	(0.1, 0, 0.9, 0)
4	N AND VH	(0.7, 0, 0.3, 0)
5	M AND N	(0.5, 0, 0.5, 0)
6	M AND M	(0.5, 0.5, 0, 0)
7	M AND H	(0, 1, 0, 0)
8	M AND VH	(0, 0, 0.5, 0.5)
9	H AND N	(0.7, 0, 0.3, 0)
10	H AND M	(0, 0.4, 0.6, 0)
11	H AND H	(0, 0, 1, 0)
12	H AND VH	(0, 0, 0.5, 0.5)
13	VH AND N	(0, 0, 0, 1)
14	VH AND M	(0.1, 0, 0.9, 0)
15	VH AND H	(0, 0, 1, 0)
16	VH AND VH	(0.5, 0, 0, 0.5)

In order to reach a prediction result with more accuracy, the initial parameter given by expert knowledge is optimized by algorithm CMA-ES, which select 150 data in each health state feature as training data, the population size is set to 40 and the iteration is 500. The updated parameters of the time series are shown in Tables 3 and 4.

**Table 3.** The updated parameters of belief rule base (BRB)-1.

Number	$x(t)$ AND $x(t-1)$	Belief Degree <sup>{<math>D_1, D_2, D_3, D_4</math>}</sup>
1	N AND N	(0.626783, 0.172457, 0.192209, 0.008551)
2	N AND M	(0.728580, 0.175145, 0.031722, 0.064553)
3	N AND H	(0.556139, 0.272169, 0.042038, 0.129654)
4	N AND VH	(0.162512, 0.229010, 0.157799, 0.450679)
5	M AND N	(0.322767, 0.153216, 0.240033, 0.283984)
6	M AND M	(0.506735, 0.191413, 0, 0.303065)
7	M AND H	(0.043160, 0.070414, 0.694565, 0.191861)
8	M AND VH	(0.145286, 0.181737, 0.116378, 0.556599)
9	H AND N	(0.147285, 0.157746, 0.225319, 0.469650)
10	H AND M	(0.213948, 0.198086, 0.323453, 0.264513)
11	H AND H	(0.257935, 0.475565, 0.113234, 0.153266)
12	H AND VH	(0.369449, 0.216516, 0.252135, 0.161900)
13	VH AND N	(0.176878, 0.462870, 0.221216, 0.139036)
14	VH AND M	(0.063354, 0.214438, 0.389715, 0.332493)
15	VH AND H	(0.022360, 0.066674, 0.140649, 0.770317)
16	VH AND VH	(0.272171, 0.312719, 0.254067, 0.161043)

**Table 4.** The updated parameters of BRB-2.

Number	$x(t)$ AND $x(t-1)$	Belief Degree <sup>{<math>D_1, D_2, D_3, D_4</math>}</sup>
1	N AND N	(0.004575, 0.681227, 0.186568, 0.127630)
2	N AND M	(0.814169, 0.099244, 0.032949, 0.053638)
3	N AND H	(0.768632, 0.229775, 0.000797, 0.000796)
4	N AND VH	(0.011045, 0.235602, 0.365752, 0.387601)
5	M AND N	(0.430231, 0.001520, 0.310416, 0.257833)
6	M AND M	(0.359677, 0.019029, 0.300818, 0.320476)
7	M AND H	(0.595030, 0.212968, 0.048263, 0.143739)
8	M AND VH	(0.397879, 0.527427, 0.010489, 0.064204)
9	H AND N	(0.254057, 0.228871, 0.399035, 0.118037)
10	H AND M	(0.110210, 0.007912, 0.288896, 0.592982)
11	H AND H	(0.170163, 0.047206, 0.504182, 0.278449)
12	H AND VH	(0.467217, 0.174257, 0.302473, 0.056053)
13	VH AND N	(0.129582, 0.287104, 0.391517, 0.191796)
14	VH AND M	(0.004112, 0.219503, 0.154751, 0.621634)
15	VH AND H	(0, 0.003267, 0, 0.996833)
16	VH AND VH	(0.080410, 0.080022, 0.345580, 0.493988)

All the data are taken as the test data to predict the health state feature of the gas path system. The results of the two health state features are shown in Figures 5 and 6. It can be seen from the diagram that the time series prediction results of health state feature optimized by CMA-ES algorithm can effectively make up for the low prediction accuracy of the health state feature results caused by the subjectivity of expert knowledge.

According to the root mean square error in Table 5, the updated result of the gas path system's health state feature is more accurate than the initial prediction result.

**Table 5.** The root mean squared error (RMSE) of different health state features.

	Initial Model	Updated Model
Health state feature 1	13.5141	12.6166
Health state feature 2	1.9534	1.5871

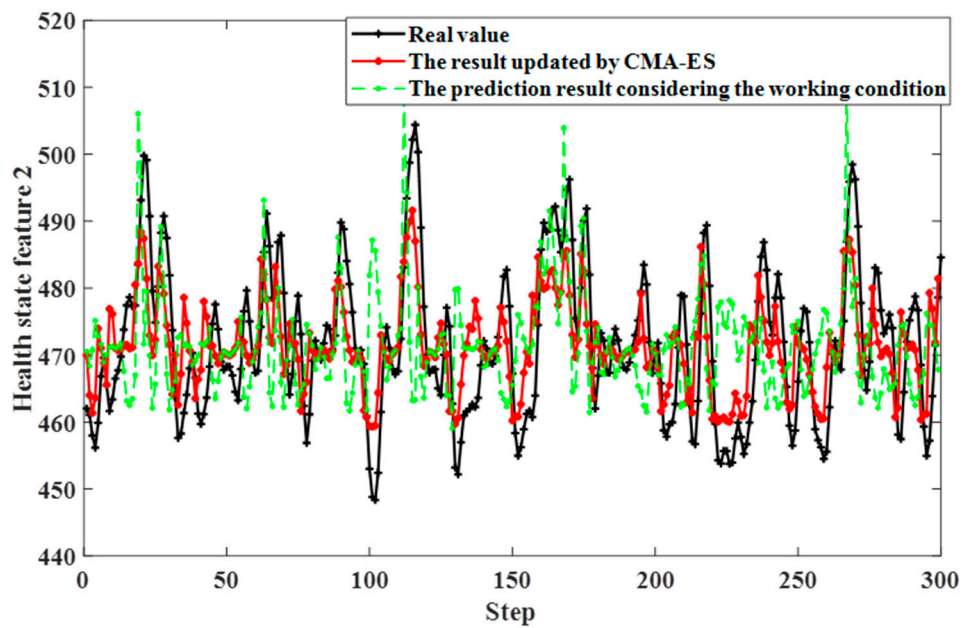


Figure 5. Prediction result of health state feature 1 in time series.

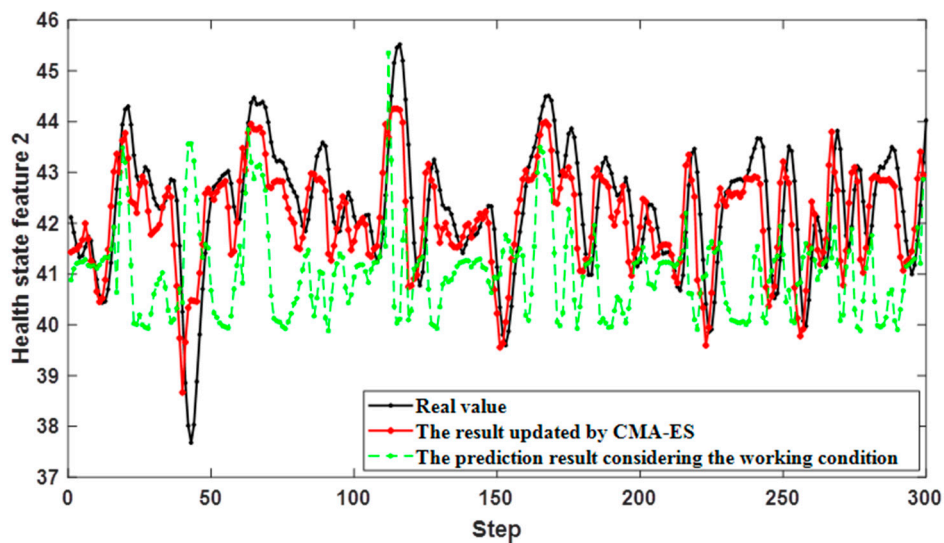


Figure 6. Prediction result of health state feature 2 in time series.

#### 4.3. Health State Prediction of Aero-Engine Gas Path System Based on BRB

The semantic value of gas path system’s health states is quantified  $(D_0, D_1, D_2, D_3, D_4) = (1, 0.75, 0.50, 0.25, 0)$ , where  $D_i$  is the different health states of gas path system,  $F_i$  is the health state feature of gas path system. The health state prediction model of the gas path system is shown in Equation (29).

$$R_k^q : \text{If } F_1 \text{ is } A_1^k \wedge F_2 \text{ is } A_2^k \text{ Then the health state is } \{(D_0, \beta_{1,k}), (D_1, \beta_{2,k}), (D_3, \beta_{3,k}), (D_4, \beta_{4,k}), (D_5, \beta_{5,k})\} \quad (29)$$

with a rule weight  $\theta_k$  and attribute weight  $\delta_1, \delta_2, \delta_3, \delta_4, \delta_5$

where,  $A_1^k$  and  $A_2^k$  respectively represent the reference values of two health state characteristic quantities under condition  $P$ .

The health state prediction results of BRB-1 and BRB-2 are taken as the input of BRB-3, which can predict the health states of the aero-engine gas path system. The reference values

of the two health state features are shown in Table 1. There are 16 rules of the gas path system’s health state prediction model because the number of two health state features’ reference points is 4. The initial parameters given by expert knowledge are shown in Table 6.

**Table 6.** The updated parameters of BRB-2.

Number	$x(t)$ AND $x(t-1)$	Belief Degree <sup>{D<sub>1</sub>,D<sub>2</sub>,D<sub>3</sub>,D<sub>4</sub>}</sup>
1	N AND N	(1, 0, 0, 0,0)
2	N AND M	(0, 0, 0.7, 0.3, 0)
3	N AND H	(0, 0, 0, 0.8, 0.2)
4	N AND VH	(0.9, 0, 0, 0, 0.1)
5	M AND N	(0, 0.5, 0.5, 0, 0)
6	M AND M	(0, 0, 0.5, 0.5, 0)
7	M AND H	(0, 0, 0, 0.5, 0.5)
8	M AND VH	(0, 0.5, 0, 0, 0.5)
9	H AND N	(0.3, 0, 0, 0.7, 0)
10	H AND M	(0.2, 0, 0, 0.8, 0)
11	H AND H	(0.4, 0, 0, 0.6, 0)
12	H AND VH	(0.1, 0, 0, 0, 0.9)
13	VH AND N	(0, 0.1, 0.9, 0, 0)
14	VH AND M	(0, 0, 0.2, 0.8, 0)
15	VH AND H	(0, 0, 0, 0.3, 0.7)
16	VH AND VH	(0.3, 0, 0, 0, 0.7)

In order to make up the subjectivity of expert knowledge, the CMA-ES optimization algorithm is used to optimize the parameters given by expert knowledge where the number of the population is set to 66, and the number of iterations is set to 100. The optimized parameters are shown in Table 7. The health state prediction results are shown in Figure 7.

**Table 7.** The updated parameters of BRB-2.

Number	$x(t)$ AND $x(t-1)$	Belief Degree <sup>{D<sub>1</sub>,D<sub>2</sub>,D<sub>3</sub>,D<sub>4</sub>}</sup>
1	N AND N	(0.221159, 0.28597, 0.086321, 0.062829, 0.343714)
2	N AND M	(0.128107, 0.003393, 0.203260, 0.022314, 0.642926)
3	N AND H	(0.254224, 0.251018, 0.290395, 0.161309, 0.043054)
4	N AND VH	(0.134931, 0.210087, 0.466548, 0.144023, 0.044411)
5	M AND N	(0.865790, 0.048182, 0, 0.071426, 0.025662)
6	M AND M	(0.100423, 0.072713, 0.098077, 0.178782, 0.550006)
7	M AND H	(0.005379, 0.308059, 0.459540, 0.121880, 0.105142)
8	M AND VH	(0.253789, 0.048157, 0.262505, 0.335647, 0.099902)
9	H AND N	(0.193258, 0.302860, 0.149030, 0.160192, 0.194660)
10	H AND M	(0.536648, 0.316348, 0.041354, 0.094337, 0.011313)
11	H AND H	(0.046835, 0.280231, 0.201947, 0.205796, 0.265191)
12	H AND VH	(0.665204, 0.094559, 0.195134, 0.035089, 0.010013)
13	VH AND N	(0.100497, 0, 0.611047, 0.287832, 0.013454)
14	VH AND M	(0.020941, 0.071357, 0.417684, 0.102784, 0.387233)
15	VH AND H	(0.237159, 0.214191, 0.199517, 0.211400, 0.137733)
16	VH AND VH	(0.492739, 0.255117, 0, 0.121081, 0.143010)

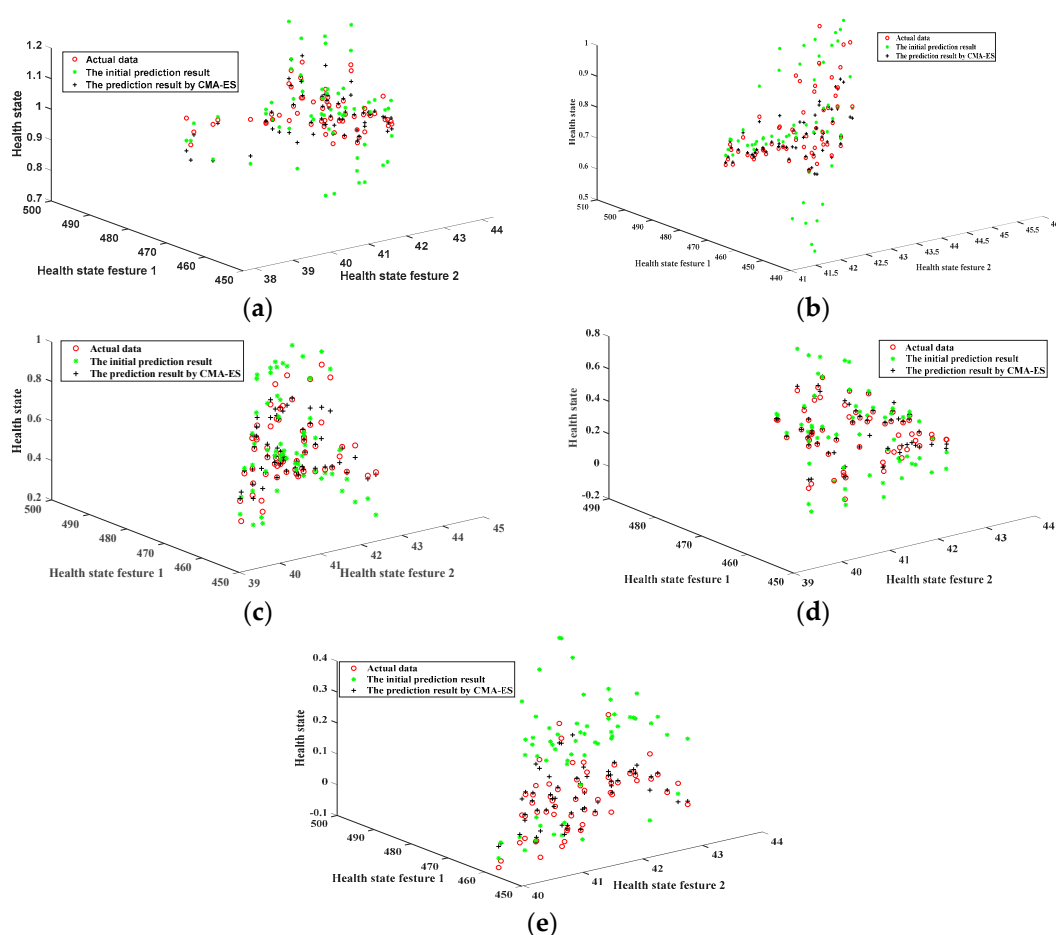


**Figure 7.** (a) Health state prediction result under working condition 1; (b) health state prediction result under working condition 2; (c) health state prediction result under working condition 3; (d) health state prediction result under working condition 4; (e) health state prediction result under working condition 5.

The health state prediction results of the gas path system under the different working conditions are shown in Figure 8. According to the health state prediction result of Figure 8, the updated prediction result can better predict the health states under different working conditions. In order to reflect the health state prediction results of gas path system, the above five health state prediction result under different working conditions are integrated, which is shown in Figure 8.

The health state prediction result updated by CMA-ES optimization algorithm is more accurate by calculating the root mean square error, which is shown in Table 8.

**Table 8.** The RMSE of different health state prediction model.

Prediction Model	Initial Model	Updated Model
RMSE	2.4001	1.1341

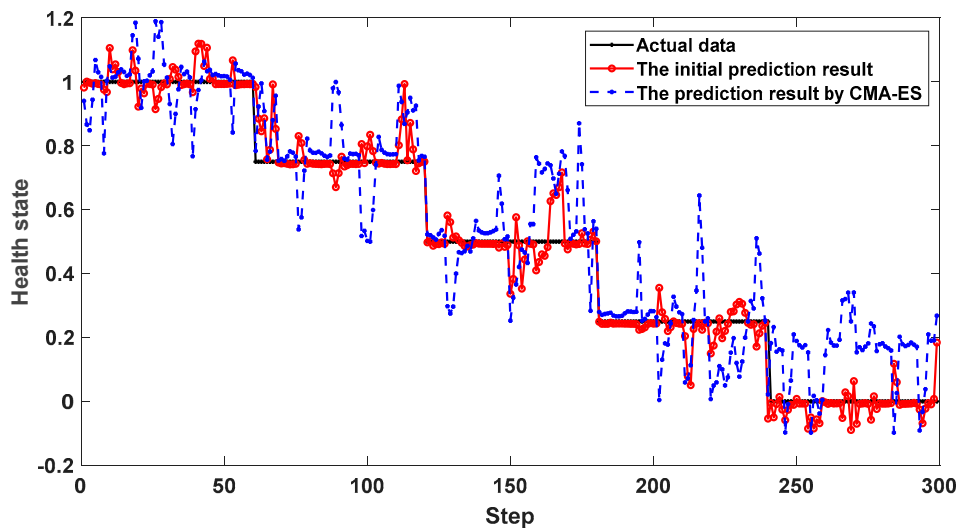


Figure 8. Health state prediction result in whole system.

4.4. Comparative Analysis

In order to verify the accuracy of the gas path system’s health state prediction model, the health state prediction model without the consideration of the multiple working conditions is taken as a comparison. The reference points of the two health state features are shown in Table 9, and the initial belief parameters are shown in Table 2.

Table 9. The reference points without considering the multiple working conditions.

Semantic Value	N	M	H	VH
Health state feature 1	448	467	486	505
Health state feature 2	37.67	40.29	42.91	45.52

In order to account for the subjectivity of expert knowledge, the CMA-ES optimization algorithm is used to optimize the initial parameters of health state features in time series, which are shown in Tables 10 and 11.

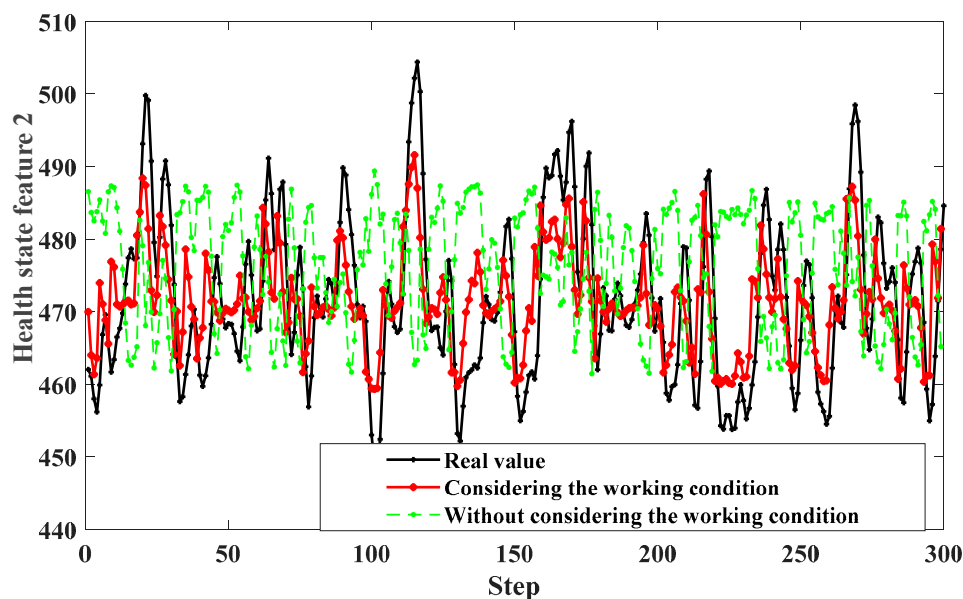
Table 10. The updated parameters of BRB-1 without considering the working condition.

Number	$x(t)$ AND $x(t-1)$	Belief Degree <sup>{D<sub>1</sub>,D<sub>2</sub>,D<sub>3</sub>,D<sub>4</sub>}</sup>
1	N AND N	(0.153716, 0.292718, 0.105993, 0.447573)
2	N AND M	(0.861800, 0.070716, 0.067365, 0.000119)
3	N AND H	(0.321176, 0.232704, 0.087782, 0.358338)
4	N AND VH	(0.005139, 0.203536, 0.719891, 0.071434)
5	M AND N	(0.292742, 0.071456, 0.142251, 0.493551)
6	M AND M	(0.235056, 0.338192, 0.184549, 0.242203)
7	M AND H	(0.570791, 0.234295, 0.114994, 0.079920)
8	M AND VH	(0.166535, 0.134635, 0.246974, 0.451856)
9	H AND N	(0.584955, 0.113851, 0.201512, 0.099682)
10	H AND M	(0.254735, 0.140327, 0.156385, 0.448553)
11	H AND H	(0.195430, 0.316090, 0.126253, 0.362226)
12	H AND VH	(0.295834, 0.296295, 0.362953, 0.044918)
13	VH AND N	(0.131752, 0.187740, 0.354663, 0.325845)
14	VH AND M	(0, 0.184149, 0.105118, 0.733013)
15	VH AND H	(0.169244, 0.187260, 0.193144, 0.450352)
16	VH AND VH	(0.087349, 0.047340, 0.118129, 0.747182)

**Table 11.** The updated parameters of BRB-2 without considering the working condition.

Number	$x(t)$ AND $x(t-1)$	Belief Degree <sup>{D<sub>1</sub>,D<sub>2</sub>,D<sub>3</sub>,D<sub>4</sub>}</sup>
1	N AND N	(0.498411, 0.132257, 0.193689, 0.175643)
2	N AND M	(0.611554, 0.259469, 0.034879, 0.094098)
3	N AND H	(0.064522, 0.276302, 0.519704, 0.139472)
4	N AND VH	(0.045459, 0.434752, 0.425926, 0.093863)
5	M AND N	(0.113100, 0.532354, 0.197630, 0.156916)
6	M AND M	(0.209847, 0.367045, 0.038525, 0.384583)
7	M AND H	(0.446034, 0.131154, 0.171720, 0.251092)
8	M AND VH	(0.502878, 0.389269, 0.102874, 0.004980)
9	H AND N	(0.334728, 0.054691, 0.424291, 0.186290)
10	H AND M	(0, 0.305871, 0.350689, 0.361470)
11	H AND H	(0.148548, 0.195574, 0.248609, 0.4072689)
12	H AND VH	(0.283669, 0.443720, 0.156855, 0.115755)
13	VH AND N	(0.336328, 0.258820, 0.231363, 0.173489)
14	VH AND M	(0.195087, 0.332693, 0.290819, 0.181401)
15	VH AND H	(0.106367, 0.026548, 0.0913323, 0.775752)
16	VH AND VH	(0.155854, 0.281593, 0.317729, 0.244824)

The health state prediction result of the two health state features without considering the multiple working conditions are shown in Figures 9 and 10.

**Figure 9.** The comparison result 1 without considering the multiple working conditions.

The health state features in a time series without considering the multiple working conditions can predict the change of the gas path system's health state features on the whole, while it cannot predict the change of health state features on the local position in more detail. The time series prediction model considering the multiple working conditions is more accurate than the health state prediction model without considering the multiple working conditions, which is shown in Table 12.

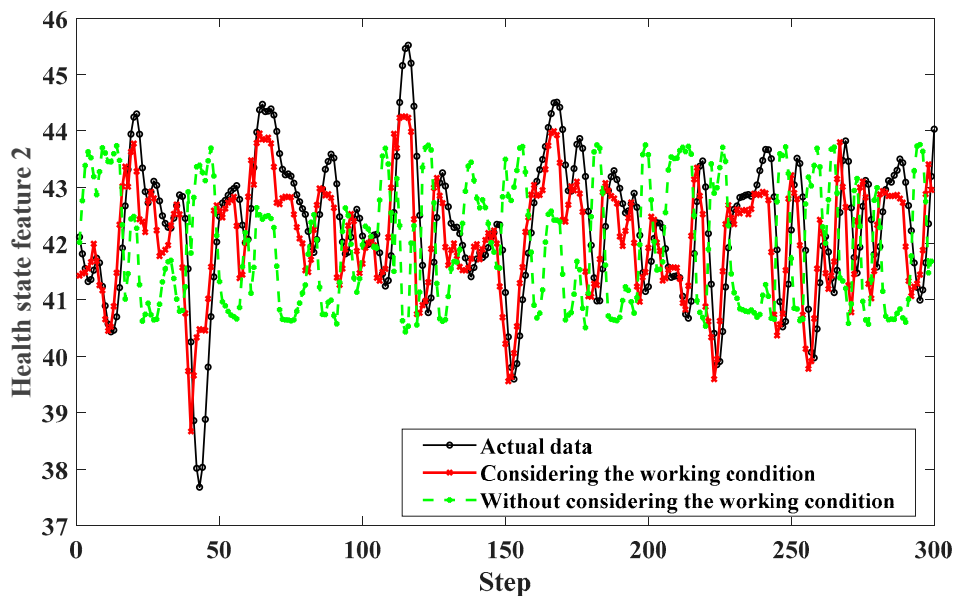


Figure 10. The comparison result 2 without considering the multiple working conditions.

Table 12. The RMSE of different health state prediction model.

	Without the Working Condition	Considering the Working Condition
Health state feature 1	14.5066	12.6166
Health state feature 2	1.6507	1.5871

Based on the above prediction results of the health state characteristic quantity, the health state prediction of the gas path system is carried out.

The health state prediction model of gas path system is established based on the above prediction result of health state features and the reference points are the same as the health state prediction model  $(D_0, D_1, D_2, D_3, D_4) = (1, 0.75, 0.50, 0.25, 0)$ . The updated parameters are shown in Table 13.

Table 13. The updated parameters of BRB-3 without considering the working condition.

Number	$x(t)$ AND $x(t-1)$	Belief Degree <sup><math>(D_1, D_2, D_3, D_4)</math></sup>
1	N AND N	(0, 0.067471, 0.444641, 0.412738, 0.07515)
2	N AND M	(0.284484, 0.306296, 0.217246, 0.191974, 0)
3	N AND H	(0.283654, 0, 0.12222, 0.282109, 0.312018)
4	N AND VH	(0.528186, 0.205603, 0.209657, 0.056554, 0)
5	M AND N	(0.837629, 0.108553, 0.02377, 0, 0.030048)
6	M AND M	(0.410296, 0.314038, 0.03181, 0, 0.243856)
7	M AND H	(0, 0.089721, 0.161532, 0.324373, 0.424373)
8	M AND VH	(0, 0.085559, 0.280462, 0.190165, 0.443814)
9	H AND N	(0.133626, 0.592918, 0.111606, 0, 0.161849)
10	H AND M	(0, 0.020687, 0.232157, 0.375878, 0.371278)
11	H AND H	(0.191792, 0.061321, 0, 0.08299, 0.663897)
12	H AND VH	(0.247792, 0.321502, 0, 0.132951, 0.297755)
13	VH AND N	(0.206588, 0, 0.149312, 0.246661, 0.397439)
14	VH AND M	(0.145951, 0.180765, 0, 0.106762, 0.566522)
15	VH AND H	(0.468404, 0.268239, 0, 0.092345, 0.171013)
16	VH AND VH	(0, 0.034978, 0.051346, 0.118371, 0.795306)

There is an obvious stratification phenomenon of health state prediction without the consideration of the multiple working conditions in Figure 11, while it can predict the real health states of the gas path system.

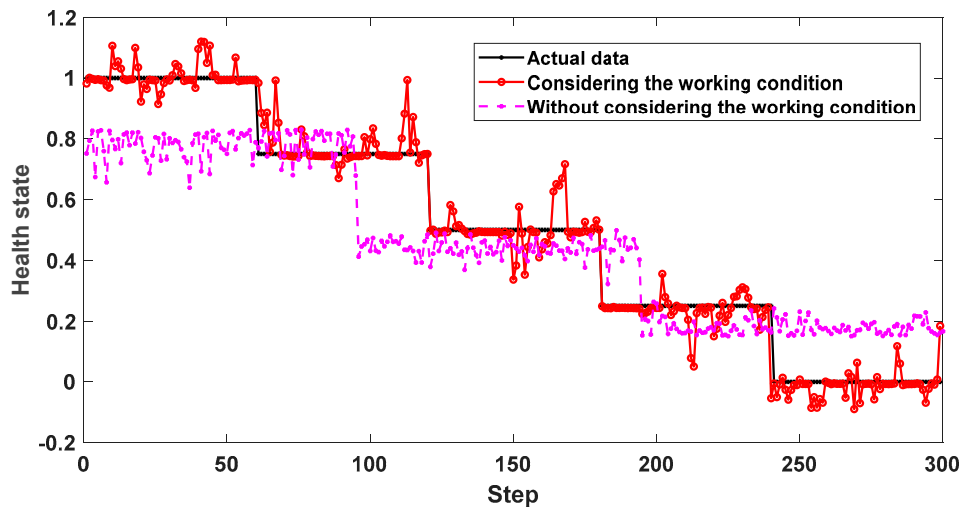


**Figure 11.** The health state prediction result without considering the multiple working conditions.

By calculating RMSE of the different health state models for gas path system, the health state prediction model with the consideration of multiple working conditions is more accurate than the health state prediction model without the consideration of multiple working conditions, which is shown in Table 14.

**Table 14.** The RMSE of different health state prediction models.

Prediction Model	Without the Working Condition	Considering the Working Condition
RMSE	3.9113	1.1314

## 5. Discussion

The results show that the health state prediction model has obvious advantages that make full use of expert knowledge given the problems of less available data and considering the working conditions for an aero-engine gas path system. Naturally, when a single working condition and a lot of data are used, the result is no different from other data-driven methods. When there are more feature data, the real-time capability of the model is poor. Now, however, we use a small amount of data and consider working conditions for research to establish a health state prediction model with short calculation time and high accuracy. In order to make up for the subjectivity of expert knowledge, we use the fuzzy C-means method to divide the reference value of the feature. In further research, more features and consideration of working condition changes should be used to build a more accurate health prediction model.

## 6. Conclusions

In this paper, health state prediction of aero-engine gas path system considering the multiple working conditions based on time domain analysis and a belief rule base is proposed. This model first solves the problem that the unitary working condition cannot accurately express the health states of the aero-engine gas circuit system, and then solves the problem that the accuracy of the model is incorrect when the expert knowledge determines the characteristic reference value. Take the NASA public data set as an example to illustrate its effectiveness.

The main contributions of this paper are as follows.

- (1) The working condition of gas path system is divided based on time-domain features. The different values are set for different health states under different working conditions and combining expert knowledge to establish a health state prediction model for an aero-engine gas circuit system, which can significantly improve the accuracy of the gas path system's health states.
- (2) In order to further improve the accuracy of the health state prediction model and make up for the subjectivity of expert knowledge, the CMA-ES optimization algorithm is used to optimize the relevant parameters in the prediction model given by experts and fuzzy c-mean is used to calculate the reference value of the feature, which can further improve the accuracy of the health state prediction model.

**Author Contributions:** Conceptualization, X.Y. and G.S.; methodology, S.P. and G.S.; software, S.P.; validation, S.P., G.S. and Y.Z.; formal analysis, S.P. and G.S.; investigation, S.P., G.S. and Y.Z.; resources, X.Y., B.Z. and W.S.; data curation, G.S.; writing—original draft preparation, S.P., G.S. and Y.Z.; writing—review and editing, X.Y. and B.Z.; visualization, X.Y. and B.Z.; supervision, X.Y., B.Z. and W.S.; project administration, X.Y. and B.Z.; funding acquisition, B.Z. and X.Y. All authors have read and agreed to the published version of the manuscript.

**Funding:** This work is supported by the National Natural Science Foundation of China under Grants 61803044, Project of the Science and Technology Department of Jilin Province of China under Grand 20200403036SF, National Natural Science Foundation of China under Grants 61973046, and Project of the Science and Technology Department of Jilin Province of China under Grand 20200301038RQ.

**Institutional Review Board Statement:** Not applicable.

**Informed Consent Statement:** Not applicable.

**Data Availability Statement:** The paper uses NASA's public data set "7.PHM08 Challenge Data Set" at <https://ti.arc.nasa.gov/tech/dash/groups/pcoe/prognostic-data-repository/>, accessed on 20 April 2020.

**Conflicts of Interest:** The authors declare that they have no known competing financial interests or personal relationships that could have appeared to influence the work reported in this paper.

## References

1. Mattingly, J.D.; Mattingly, J.D.; Mattingly, J.D. *Aircraft Engine Design*, 2nd ed; American Institute of Aeronautics and Astronautics Inc.: Reston, VA, USA, 2015.
2. Kumar, T.; Mohsin, R.; Majid, Z.A.; Ghafir, M.; Wash, A.M. Experimental study of the anti-knock efficiency of high-octane fuels in spark ignited aircraft engine using response surface methodology. *J. Appl. Energy* **2020**, *259*, 1–23. [\[CrossRef\]](#)
3. Zhang, J.J.; Wang, P.; Yan, R.Q.; Gao, R.X. Deep learning for improved system remaining life prediction. *J. Procedia CIRP* **2018**, *72*, 1033–1038. [\[CrossRef\]](#)
4. Leite, G.; Araújo, A.M.; Rosas, P. Prognostic techniques applied to maintenance of wind turbines: A concise and specific review. *J. Renew. Sustain. Energy Rev.* **2018**, *81*, 1917–1925. [\[CrossRef\]](#)
5. Qian, S.J.; Han, N.; Zhu, X.W.; Shu, H.P.; Zheng, J.L.; Yuan, C.A. A dynamic trajectory prediction algorithm based on Kalman Filter. *J. Acta Electron. Sin.* **2018**, *46*, 418–423.
6. Siavash, H. Deep Kalman Filter: Simultaneous multi-sensor integration and modelling; A GNSS/IMU case study. *J. Sens.* **2018**, *18*, 13–29.
7. Dejamkhooy, A.; Dastfan, A.; Ahmadyfard, A. Modeling and Forecasting Non-Stationary Voltage Fluctuation Based on Grey System Theory. *J. IEEE Trans. Power Deliv.* **2017**, *32*, 1212–1219. [\[CrossRef\]](#)
8. Nguyen, N.; Tran, T. Optimizing mathematical parameters of grey system theory: An empirical forecasting case of vietnamese tourism. *J. Neural Comput. Appl.* **2017**, *35*, 58–75. [\[CrossRef\]](#)
9. Bin, L. Sliding model controller design for joint servo of apple harvesting robot based on grey theory. *J. Agric. Mech. Res.* **2017**, *32*, 1212–1219.
10. Wang, X.; Evans, D.; Yu, Q. Feature squeezing: Detecting adversarial examples in deep neural networks. In Proceedings of the Network and Distributed System Security Symposium, San Diego, CA, USA, February 26–March 1 2017.
11. Jiang, D.X.; Wang, F.Y.; Zhou, M.; Wei-Dou, N.I. Application of fuzzy self-organizing neural network to aero-engine fault diagnosis. *J. Aerosp. Power* **2001**, *16*, 80–82.
12. Gang, Y.; Huang, J.Q. Aero-engine fault diagnosis based on support vector machine and Kalman Filter. *J. Aeroengine* **2012**, *38*, 47–50.
13. Bagherzadeh, S.A. Nonlinear aero elastic modeling of aircraft using support vector machine method. *J. Aircr. Eng. Aerosp. Technol.* **2020**, *92*, 502–518. [\[CrossRef\]](#)

14. Zeng, Z.F.; Xiao, X.; Cui, Y. Principles of methodology engineering in HAD. *J. Aeronaut. Comput. Technol.* **2007**, *37*, 73–74.
15. Zhong, S.S.; Luan, S.G. Aeroengine condition monitoring and maintenance data processing system oriented to lifecycle management. *J. Comput. Integr. Manuf. Syst.* **2006**, *12*, 10–25.
16. Zhang, B.; Li, Y.; Bai, Y.; Cao, Y. Aero engines remaining useful life prediction based on improved C-Loss ELM. *J. IEEE Access* **2020**, *16*, 49752–49764. [[CrossRef](#)]
17. Cui, J.; Gao, B.; Jiang, L.; Yu, M.Y.; Zheng, W.; Automation, S.O.; University, S.A. Application research of LSSVM and HMM in aero engine condition prediction. *J. Comput. Eng.* **2017**, *66*, 6512–6528.
18. Yin, X.; Wang, Z.; Zhang, B.; Zhou, Z.; Gao, Z. Health estimation of fan based on belief-rule-base expert system in turbofan engine gas-path. *J. Adv. Mech. Eng.* **2017**, *6*, 12–28. [[CrossRef](#)]
19. Wallace, M.C.; Britton, S.T.; Meek, R. Comparison of five video-assisted intubation devices by novice and expert laryngoscopists for use in the aeromedical evacuation environment. *J. Mil. Med Res.* **2017**, *16*, 49752–49764. [[CrossRef](#)] [[PubMed](#)]
20. Mohammed, I.; Abu Talib, A.R. Mechanical properties of carbon fiber reinforced aluminium laminates using two different layering pattern for aero engine application. *J. Adv. Mater. Process. Technol.* **2019**, *5*, 123–131.
21. Liu, L.J.; Jiang, P.; Lu, F. An Intelligent Prediction Method of Aero-Engine Gas Path Performance Parameters. *J. Inst. Eng. Ind. Ser.* **2021**, *102*, 595–602. [[CrossRef](#)]
22. Zhang, Y.Z. *Study on Aeroengine Gas Parameters Prediction Based on Ensemble Learning*; D. Harbin Institute of Technology: Harbin, China, 2017.
23. Luan, S.G. *Aeroengine Condition Monitoring Technique and System Based on Gas Path Parameter Sample*; D. Harbin Institute of Technology: Harbin, China, 2008.
24. Wei, Y. *Aeroengine Condition Prediction Based on Information Fusion*; D. Harbin Institute of Technology: Harbin, China, 2014.
25. Xiong, Y.; Cheng, F.; Yongbin, L.I.; Chen, C.; Shen, J. Failure analysis of GH4033 nickel based alloy coupling ring of an aircraft engine. *J. Mater. Mech. Eng.* **2019**, *42*, 1498–1504.
26. Chen, X.X.; Qian, Y.; Sheng, G.H.; Jiang, X.C.; Man, Y.Y.; Xi, X.G. Study of UHF partial discharge sensor time domain parameters based on frequency domain deconvolution. *J. High Volt. Eng.* **2015**, *41*, 1488–1494.
27. Qin, A.; Hu, Q.; Lv, Y.; Zhang, Q. Concurrent fault diagnosis based on Bayesian discriminating analysis and time series analysis with dimensionless parameters. *J. IEEE Sens. J.* **2019**, *19*, 254–265. [[CrossRef](#)]
28. Cao, Y.; Liu, M.; Yang, J.; Cao, Y.; Fu, W. A method for extracting weak impact signal in NPP based on adaptive morlet wavelet transform and kurtosis. *J. Prog. Nucl. Energy* **2018**, *10*, 211–220. [[CrossRef](#)]
29. Zhou, Z.J.; Chang, L.L.; Hu, C.H.; Han, X.X.; Zhou, Z.G. A new BRB-ER-based model for assessing the lives of products using both failure data and expert knowledge. *J. IEEE Trans. Syst. Man Cybern. Syst.* **2015**, *12*, 1529–1543. [[CrossRef](#)]
30. Zhou, Z.J.; Hu, C.H.; Chen, Y.W. *Evidence Reasoning Belief Rule Base and Complex System Modeling*, 1st ed.; Science Press: Beijing, China, 2011.
31. Roman, R.C.; Precup, R.E.; Petriu, E.M. Hybrid data-driven fuzzy active disturbance rejection control for tower crane systems. *Eur. J. Control* **2001**, *58*, 373–387. [[CrossRef](#)]
32. Hou, Z.S.; Xiong, S.S. On model free adaptive control and its stability analysis. *IEEE Trans. Autom. Control* **2019**, *64*, 1–14. [[CrossRef](#)]
33. Pal, N.R.; Pal, K.; Keller, J.M.; Bezdek, J.C. A possibilistic fuzzy c-means clustering algorithm. *IEEE Trans. Fuzzy Syst.* **2005**, *13*, 517–530. [[CrossRef](#)]
34. Chen, R.; Qiu, C.X. Seismic response analysis of multi-story steel frames using BRB and SCB hybrid Bracing System. *J. Appl. Sci.* **2019**, *16*, 284. [[CrossRef](#)]
35. Yang, W.; Yue, Z.; Li, L.; Yang, F.; Wang, P. Optimization design of unitized panels with stiffeners in different formats using the evolutionary strategy with covariance matrix adaptation. *J. Proc. Inst. Mech. Eng.* **2017**, *15*, 23–33. [[CrossRef](#)]
36. Ito, K. Gaussian filter for nonlinear filtering problems. In Proceedings of the 39th IEEE Conference on Decision & Control, Sydney, Australia, 12–15 December 2000; Volume 2, pp. 1218–1223.